CRITICAL SURFACE OF THE HEXAGONAL POLYGON MODEL

GEOFFREY R. GRIMMETT AND ZHONGYANG LI

ABSTRACT. The polygon model studied here arises in a natural way via a transformation of the 1-2 model on the hexagonal lattice, and it is related to the high temperature expansion of the Ising model. There are three types of edge, and three corresponding parameters $\epsilon_a, \epsilon_b, \epsilon_c > 0$. By studying a certain two-edge correlation function, it is shown that the parameter space $(0, \infty)^3$ may be divided into *subcritical* and *supercritical* regions, separated by critical surfaces satisfying an explicitly known formula. This result complements earlier work of Grimmett and Li on the 1-2 model. The proof uses the Pfaffian representation of Fisher, Kasteleyn, and Temperley for the counts of dimers on planar graphs.

1. INTRODUCTION

The polygon model studied here is a process of statistical mechanics on the space of unions of closed loops on the hexagonal lattice $\mathbb{H}$. It arises naturally in the study of the 1-2 model, and indeed the main result of the current paper is complementary to the exact calculation of the critical surface of the 1-2 model reported in [4, 5] (to which the reader is referred for background and current theory of the 1-2 model). The polygon model may in addition be viewed as an asymmetric version of the $O(n)$ model with $n = 1$ (see [2] for a recent reference to the $O(n)$ model).

Let $G = (V, E)$ be a finite subgraph of $\mathbb{H}$. The configuration space Σ_G of the polygon model is the set of all subsets S of E such that every vertex in V is incident to an even number of members of S. The probability measure is a three-parameter product measure conditioned on belonging to Σ_G, in which the parameters are associated with the three classes of edge (see Figure 2.1).

This model may be regarded as the high temperature expansion of a certain inhomogenous Ising model on the hexagonal lattice. The latter is a special case of the general eight-vertex model of Lin and Wu [15]. Whereas Lin and Wu prove a connection between their eight-vertex model and a general Ising model, the current

Date: 29 August 2015.

2010 *Mathematics Subject Classification.* 82B20, 60K35, 05C70.

Key words and phrases. Polygon model, 1-2 model, high temperature expansion, dimer model, perfect matching, Kasteleyn matrix.

paper utilizes the additional symmetries of the current model to identify an order parameter, and thence to calculate in closed form the parametric form of the critical surface.

The order parameter used in this paper is the one that occurs naturally within the context of the Ising model, namely, the ratio $Z_{G,e\leftrightarrow f}/Z_G$, where $Z_{G,e\leftrightarrow f}$ is the partition function for configurations that include a path between two edges e, f, and Z_G is the usual partition function. This ratio may be expressed in terms of certain dimer-counts, and hence (by classical results of Kasteleyn [6, 7], and Temperley and Fisher [18]) in terms of Pfaffians of certain antisymmetric matrices. The squares of these Pfaffians are determinants, and these converge as $G \uparrow \mathbb{H}$ to the determinants of infinite block Toeplitz matrices. The limits are analytic except for certain parameter values determined by the spectral curve of the dimer model, and this enables an explicit computation of the critical surface of the polygon model.

The results of the current paper bear resemblance to earlier results of [5], in which the same authors determine the critical surface of the 1-2 model. The outline shape of the main proof (of Theorem 2.2) is similar to that of the corresponding result of [5]. In contrast, neither result seems to imply the other, and the dimer correspondence and associated calculations of the current paper are based on a different dimer representation from that of [5].

The characteristics of the hexagonal lattice that are special for this work include the properties of trivalence, planarity, and support of a $\mathbb{Z}^2$ action. It may be possible to extend the results to other such graphs, such as the Archimedean $(3, 12^2)$ lattice, and the square/octagon $(4, 8^2)$ lattice.

This article is organized as follows. The polygon model is defined in Section 2, and the main Theorem 2.2 is given in Section 2.3. The relationship between the polygon model and the 1-2 model, the Ising model, and the dimer model is explained in Section 3. The characteristic polynomial of the corresponding dimer model is calculated in Section 3.5, and Theorem 2.2 is proved in Section 4.

2. The polygon model

We begin with a description of the polygon model. Its relationship to the 1-2 model is explained in Section 3.1. The main result (Theorem 2.2) is given in Section 2.3.

2.1. **Definition of the polygon model.** Let the graph $G = (V, E)$ be a finite connected subgraph of the hexagonal lattice $\mathbb{H} = (\mathbb{V}, \mathbb{E})$, suitably embedded in $\mathbb{R}^2$ as in Figure 2.1. The embedding of $\mathbb{H}$ is chosen in such a way that each edge may be viewed as one of: horizontal, NW/SE, or NE/SW. (Later we shall consider a finite box with toroidal boundary conditions.)

Let Π be the product space $\Pi = \{0,1\}^E$. The sample space of the polygon model is the subset $\Pi^{\text{poly}} = \Pi^{\text{poly}}(G)$ of Π containing all $\pi = (\pi_e : e \in E) \in \Pi$ such that

$$\sum_{e \ni v} \pi_e \quad \text{is either 0 or 2,} \qquad v \in V. \tag{2.1}$$

Each $\pi \in \Pi^{\text{poly}}$ may be considered as a union of vertex-disjoint cycles of G, together with isolated vertices. We identify $\pi \in \Pi$ with the set $\{e \in E : \pi_e = 1\}$ of 'open' edges under π. Thus (2.1) requires that every vertex is incident to an even number of open edges.

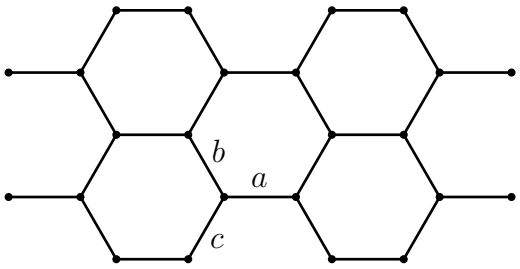

FIGURE 2.1. An embedding of the hexagonal lattice. Horizontal edges are said to be of type a, NW/SE edges of type b, and NE/SW edges of type c.

Each edge of G is allocated a type g for some $g \in \{a, b, c\}$; the type of an edge depends on its compass bearing, as indicated in Figure 2.1. Let $\epsilon_a, \epsilon_b, \epsilon_c \neq 0$. To the configuration $\pi \in \Pi^{\text{poly}}$, we assign the weight

$$w(\pi) = \prod_{e \in E} \epsilon_a^{2|\pi(a)|} \epsilon_b^{2|\pi(b)|} \epsilon_c^{2|\pi(c)|}, \tag{2.2}$$

where $\pi(s)$ is the set of open s-type edges of π. The weight function w gives rise to the partition function

$$Z_G(P) = \sum_{\pi \in \Pi^{\text{poly}}} w(\pi). \tag{2.3}$$

This, in turn, gives rise to a probability measure on Π^{poly} given by

$$\mathbb{P}_G(\pi) = \frac{1}{Z_G(P)} w(\pi), \qquad \pi \in \Pi^{\text{poly}}. \tag{2.4}$$

The measure $\mathbb{P}_G$ may be viewed as a product measure conditioned on the outcome lying in Π^{poly}. We concentrate here on an order parameter to be given next.

It is convenient to view the polygon model as a model on half-edges. To this end, let $AG = (AV, AE)$ be the graph derived from $G = (V, E)$ by adding a vertex at the

midpoint of each edge in E. Let $ME = \{Me : e \in E\}$ be the set of such midpoints, and $AV = V \cup MV$. The edges AE are precisely the half-edges of E, each being of the form $\langle v, Me\rangle$ for some $v \in V$ and incident edge $e \in E$. A polygon configuration on G induces a polygon configuration on AG, which may be described as a subset of AE with the property that every vertex in AV has even degree. For an a-type edge $e \in E$, the two half-edges of e are assigned weight ϵ_a (and similarly for b- and c-type edges). The weight function w of (2.2) may now be expressed as

$$w(\pi) = \prod_{e \in AE} \epsilon_a^{|\pi(a)|} \epsilon_b^{|\pi(b)|} \epsilon_c^{|\pi(c)|}, \qquad \pi \in \Pi^{\mathrm{poly}}(AG). \tag{2.5}$$

We introduce next the order parameter of the polygon model. Let $e, f \in ME$ be distinct midpoints of AG, and let $\Pi_{e,f}$ be the subset of all $\pi \in \{0,1\}^{AE}$ such that: (i) every $v \in AV$ with $v \neq e, f$ is incident to an even number of open half-edges, and (ii) the midpoints of e and f are incident to exactly one open half-edge. We define the order parameter as

$$M_G(e, f) = \frac{Z_{G,e\leftrightarrow f}}{Z_G(P)}, \tag{2.6}$$

where

$$Z_{G,e\leftrightarrow f} := \sum_{\pi \in \Pi_{e,f}} \epsilon_a^{|\pi(a)|} \epsilon_b^{|\pi(b)|} \epsilon_c^{|\pi(c)|}. \tag{2.7}$$

Remark 2.1. *The weight functions of* (2.2) *and* (2.5) *are unchanged under the sign change $\epsilon_g \to -\epsilon_g$ for $g = a, b, c$. Similarly, if the edges e and f have the same type, then, for $\pi \in \Pi_{e,f}$, the weight $\epsilon_a^{|\pi(a)|} \epsilon_b^{|\pi(b)|} \epsilon_c^{|\pi(c)|}$ of* (2.7) *is unchanged under this sign change. Therefore, if e and f have the same type, the order parameter $M_G(e, f)$ is independent of the sign of the ϵ_g.*

If the ϵ_g satisfy $|\epsilon_g| < 1$, the polygon model with weight function (2.5) is immediately recognized as the high temperature expansion of an inhomogeneous Ising model on AG in which the edge-interaction J_g of a g-type half-edge satisfies $\tanh J_g = |\epsilon_g|$. Indeed, under this condition, the order parameter $M_G(e, f)$ of (2.6) is simply a two-point correlation function of the Ising model. If the $|\epsilon_h|$ are sufficiently small, this Ising model is subcritical, whence $M_G(e, f)$ tends to zero in the double limit as $G \uparrow \mathbb{H}_n$ and $|e - f| \to \infty$, in that order. See [1, p. 75] and [16, 20] for accounts of the high temperature expansion, and [3] for a recent related paper.

The above Ising model may be viewed as a special case of the general eight-vertex model of Lin and Wu [15]. It is studied further in [5, Sect. 4].

2.2. **The toroidal hexagonal lattice.** We will work mostly with a finite subgraph of $\mathbb{H}$ subject to toroidal boundary conditions. Let $n \geq 1$, and let τ_1, τ_2 be the two

shifts of $\mathbb{H}$, illustrated in Figure 2.2, that map an elementary hexagon to the next hexagon in the given directions. The pair (τ_1, τ_2) generates a $\mathbb{Z}^2$ action on $\mathbb{H}$, and we write $\mathbb{H}_n = (V_n, E_n)$ for the quotient graph of $\mathbb{H}$ under the subgroup of $\mathbb{Z}^2$ generated by the powers τ_1^n and τ_2^n. The resulting $\mathbb{H}_n$ is illustrated in Figure 2.2, and may be viewed as a finite subgraph of $\mathbb{H}$ subject to toroidal boundary conditions. We write $M_n := M_{\mathbb{H}_n}$.

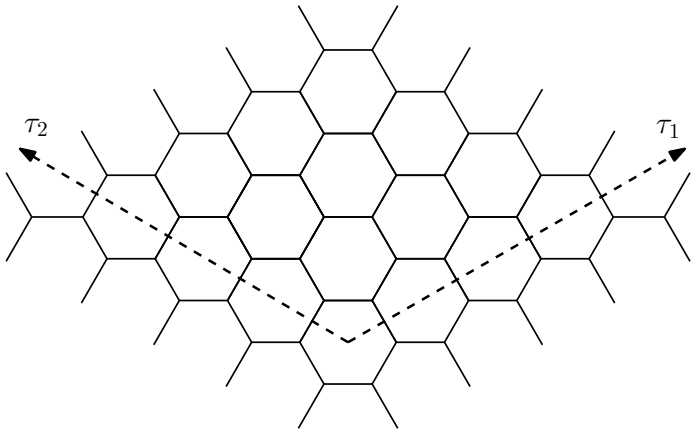

FIGURE 2.2. The graph $\mathbb{H}_n$ is an $n \times n$ 'diamond' wrapped onto a torus, as illustrated here with $n = 4$.

2.3. **Main result.** Let $e = \langle x, y \rangle$ denote the edge $e \in \mathbb{E}$ with endpoints x, y. We shall make use of a measure of distance $|e - f|$ between e and f which, for definiteness, we take to be the Euclidean distance between the midpoints of e and f, with $\mathbb{H}$ embedded in $\mathbb{R}^2$ in the manner of Figure 2.2 with unit edge-lengths.

Let

$$\alpha = \epsilon_a^2, \quad \beta = \epsilon_b^2, \quad \gamma = \epsilon_c^2. \tag{2.8}$$

Our main theorem is as follows.

Theorem 2.2. *Let $e, f \in \mathbb{E}$ be NW/SE edges such that:*

$$\begin{aligned} &\text{there exists a path } \ell = \ell(e, f) \text{ of } A\mathbb{H}_n \text{ from } Me \text{ to } Mf, \\ &\text{using only horizontal and NW/SE half-edges.} \end{aligned} \tag{2.9}$$

Let $\epsilon_g \neq 0$ for $g = a, b, c$, so that $\alpha, \beta, \gamma > 0$, and let

$$\gamma_1 = \left| \frac{1 - \alpha\beta}{\alpha + \beta} \right|, \qquad \gamma_2 = \left| \frac{1 + \alpha\beta}{\alpha - \beta} \right|, \tag{2.10}$$

where γ_2 is interpreted as ∞ if $\alpha = \beta$.

(a) *The limit* $M(e,f) = \lim_{n\to\infty} M_n(e,f)$ *exists for* $\gamma \neq \gamma_1, \gamma_2$.

(b) Supercritical case. *Let* R_{sup} *be the set of all* $(\alpha,\beta,\gamma) \in (0,\infty)^3$ *satisfying*

$$\left|\frac{1-\alpha\beta}{\alpha+\beta}\right| < \gamma < \left|\frac{1+\alpha\beta}{\alpha-\beta}\right|,$$

The limit $\Lambda(\alpha,\beta,\gamma) := \lim_{|e-f|\to\infty} M(e,f)^2$ *exists on* R_{sup}*, and satisfies* $\Lambda > 0$ *except possibly on some nowhere dense subset.*

(c) Subcritical case. *Let* R_{sub} *be the set of all* $(\alpha,\beta,\gamma) \in (0,\infty)^3$ *satisfying*

$$\textit{either} \quad \gamma < \left|\frac{1-\alpha\beta}{\alpha+\beta}\right| \quad \textit{or} \quad \gamma > \left|\frac{1+\alpha\beta}{\alpha-\beta}\right|.$$

The limit $\Lambda(\alpha,\beta,\gamma)$ *exists on* R_{sub} *and satisfies* $\Lambda = 0$.

The definitions of R_{sup} and R_{sub} are motivated by the forthcoming Proposition 3.4. Assumption (2.9) is illustrated in Figure 2.3.

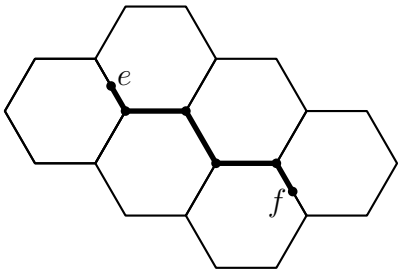

FIGURE 2.3. A path ℓ of NW/SE and horizontal edges connecting the midpoints of e and f.

Theorem 2.2 is not necessarily a complete picture of the location of critical phenomena, since e and f are assumed to satisfy condition (2.9). By Remark 2.1, it will suffice to prove Theorem 2.2 subject to the assumption that $\epsilon_g > 0$ for $g = a, b, c$.

3. The 1-2 and dimer models

We summarize next the relations between the polygon and the 1-2 and dimer models.

3.1. **The 1-2 model.** A *1-2 configuration* on the toroidal graph $\mathbb{H}_n = (V_n, E_n)$ is a subset $F \subseteq E_n$ such that every $v \in V_n$ is incident to either one or two members of F. The subset F may be expressed as a vector in the space $\Sigma_n = \{-1, 1\}^{E_n}$ where -1 represents an absent edge and 1 a present edge. Thus the space of 1-2 configurations may be viewed as the subset of Σ_n containing all vectors σ such that

$$\sum_{e \ni v} \sigma'_e \in \{1, 2\}, \qquad v \in V_n,$$

where $\sigma'_e = \frac{1}{2}(1+\sigma_e)$.

The hexagonal lattice $\mathbb{H}$ is bipartite, and we colour the two vertex-classes *black* and *white*. Let $a, b, c \geq 0$ be such that $(a,b,c) \neq (0,0,0)$, and associate these three parameters with the edges as in Figure 2.1. For $\sigma \in \Sigma_n$ and $v \in V_n$, let $\sigma|_v$ be the sub-configuration of σ on the three edges incident to v, and assign weights $w(\sigma|_v)$ to the σ_v as in Figure 3.1.

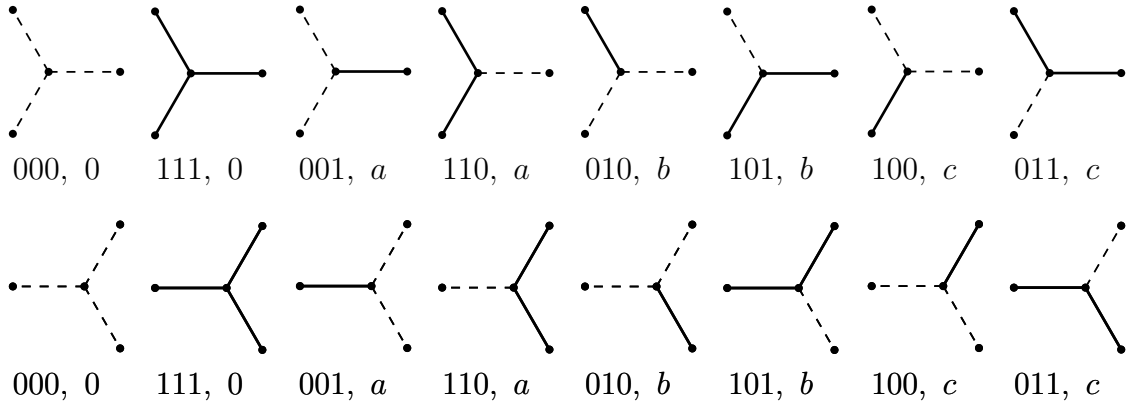

FIGURE 3.1. The eight possible local configurations $\sigma|_v$ at a vertex v in the two cases of *black* and *white* vertices (see the upper and lower figures, respectively). The signature of each is given, and also the local weight $w(\sigma|_v)$ associated with each local configuration.

Let

$$w(\sigma) = \prod_{v \in V} w(\sigma|_v), \qquad \sigma \in \Sigma_n, \tag{3.1}$$

and

$$Z_n = \sum_{\sigma \in \Sigma} w(\sigma). \tag{3.2}$$

This gives rise to the probability measure

$$\mu_n(\sigma) = \frac{1}{Z_n} w(\sigma), \qquad \sigma \in \Sigma. \tag{3.3}$$

We write $\langle X \rangle_n$ for the expectation of the random variable X with respect to μ_n.

The 1-2 model was introduced by Schwartz and Bruck [17] in a calculation of the capacity of a certain constrained coding system. It has been studied by Li [12, 14], and more recently by Grimmett and Li [5]. See [4] for a review.

3.2. **The 1-2 model as a polygon model.** By [5, Prop. 4.1], the 1-2 model with parameters a, b, c on $\mathbb{H}_n$ has partition function Z_n that differs by a smooth multiplicative constant from the partition function Z_n' given by

$$Z_n' = \sum_{\sigma\in\Sigma} \prod_{v\in V_n} \big(1 + A\sigma_{v,b}\sigma_{v,c} + B\sigma_{v,a}\sigma_{v,c} + C\sigma_{v,a}\sigma_{v,b}\big), \tag{3.4}$$

where $\sigma_{v,g}$ denotes the state of the g-type edge incident to $v \in V$, and

$$A = \frac{a-b-c}{a+b+c}, \quad B = \frac{b-a-c}{a+b+c}, \quad C = \frac{c-a-b}{a+b+c}. \tag{3.5}$$

Each $e = \langle u, v\rangle \in E_n$ contributes twice to the product in (3.4), in the forms $\sigma_{u,g}$ and $\sigma_{v,g}$ for some $g \in \{a, b, c\}$. We write σ_e for this common value, and we expand (3.4) to obtain a polynomial in the variables σ_e. In summing over $\sigma \in \Sigma$, a term disappears if it contains some σ_e with odd degree. Therefore, in each monomial $M(\sigma)$ of the resulting polynomial, every σ_e has even degree, that is, degree either 0 or 2. With the monomial M we associate the set π_M of edges e for which the degree of σ_e is 2. By examination of (3.4) or otherwise, we may see that π_M is a polygon configuration in $\mathbb{H}_n$, which is to say that the graph (V_n, π_M) comprises vertex-disjoint circuits (that is, closed paths that revisit no vertex) and isolated vertices. Indeed, there is a one-to-one correspondence between monomials M and polygon configurations π. The corresponding polygon partition function is given at (2.3) where the weights ϵ_a, ϵ_b, ϵ_c satisfy

$$\epsilon_b\epsilon_c = A, \quad \epsilon_a\epsilon_c = B, \quad \epsilon_a\epsilon_b = C, \tag{3.6}$$

which is to say that

$$\epsilon_a^2 = \frac{BC}{A}, \quad \epsilon_b^2 = \frac{AC}{B}, \quad \epsilon_c^2 = \frac{AB}{C}. \tag{3.7}$$

Note that these squares may be negative, whence the corresponding ϵ_a, ϵ_b, ϵ_c are either real or purely imaginary.

The relationship between ϵ_g and the parameters a, b, c is given in the following elementary lemma, the proof of which is omitted.

Lemma 3.1. *Let $a \geq b \geq c > 0$, and let ϵ_g be given by (3.5)–(3.7).*

(a) *Let $a < b + c$. Then $\epsilon_a, \epsilon_b, \epsilon_c$ are purely imaginary, and moreover*
  (i) *if $a^2 < b^2 + c^2$, then $0 < |\epsilon_a| < 1$, $0 < |\epsilon_b| < 1$, $0 < |\epsilon_c| < 1$,*
  (ii) *if $a^2 = b^2 + c^2$, then $|\epsilon_a| = 1$, $0 < |\epsilon_b| < 1$, $0 < |\epsilon_c| < 1$,*
  (iii) *if $a^2 > b^2 + c^2$, then $|\epsilon_a| > 1$, $0 < |\epsilon_b| < 1$, $0 < |\epsilon_c| < 1$.*

(b) *If $a = b + c$, then $|\epsilon_a| = \infty$, $\epsilon_b = \epsilon_c = 0$.*

(c) *If $a > b + c$, then $\epsilon_a, \epsilon_b, \epsilon_c$ are real, and moreover $|\epsilon_a| > 1$, $0 < |\epsilon_b| < 1$, $0 < |\epsilon_c| < 1$.*

Equations (3.6)–(3.7) express the ϵ_g in terms of A, B, C. Conversely, for given real $\epsilon_g \neq 0$, it will be useful later to define A, B, C by (3.6), even when there is no corresponding 1-2 model.

3.3. **Two-edge correlation in the 1-2 model.** Consider the 1-2 model on $\mathbb{H}_n$ with parameters a, b, c, and specifically the two-edge correlation $\langle \sigma_e \sigma_f \rangle_n$ where $e, f \in E_n$ are distinct.

We multiply through (3.4) by $\sigma_e \sigma_f$ and expand in monomials. This amounts to expanding (3.4) and retaining those monomials M in which every σ_g has even degree except σ_e and σ_f, which have degree 1. We may associate with M a set π'_M of half-edges g of $A\mathbb{H}_n$ such that: (i) the midpoints Me and Mf have degree 1, and (ii) every other vertex in AV_n has even degree. Such a configuration comprises a set of cycles together with a path between Me and Mf. The next lemma is immediate.

Lemma 3.2. *The two-edge correlation function of the 1-2 model satisfies*

$$\langle \sigma_e \sigma_f \rangle_n = \frac{Z_{n,e\leftrightarrow f}}{Z_n(P)} = M_n(e,f), \tag{3.8}$$

where the numerator $Z_{n,e\leftrightarrow f}$ is given in (2.7), and the parameters of the polygon model satisfy (3.7) and (3.5).

3.4. **The polygon model as a dimer model.** We show next a one-to-one correspondence between polygon configurations on $\mathbb{H}_n$ and dimer configurations on the corresponding *Fisher graph* of $\mathbb{H}_n$. The Fisher graph $\mathbb{F}_n$ is obtained from $\mathbb{H}_n$ by replacing each vertex by a 'Fisher triangle' (comprising three 'triangular edges'), as illustrated in Figure 3.2. A *dimer configuration* (or *perfect matching*) is a set D of edges such that each vertex is incident to exactly one edge of D.

Let π be a polygon configuration on $\mathbb{H}_n$ (considered as collection of edges). The local configuration of π at a black vertex $v \in V_n$ is one of the four configurations at the top of Figure 3.2, and the corresponding local dimer configuration is given in the lower line (a similar correspondence holds at white vertices). The construction may be expressed as follows. Each edge e of $\mathbb{F}_n$ lies either in a Fisher triangle, or it is inherited from $\mathbb{H}_n$ (that is, e is the central third of an edge of $\mathbb{H}_n$). In the latter case, we place a dimer on e if and only if $e \notin \pi$. Having applied this rule on the edges inherited from $\mathbb{H}_n$, there is a unique allocation of dimers to the triangular edges that results in a dimer configuration on $\mathbb{F}_n$. We write $D = D(\pi)$ for the resulting dimer configuration, and note that the correspondence $\pi \leftrightarrow D$ is one-to-one.

By (2.2), the weight $w(\pi)$ is the product (over $v \in V_n$) of a local weight at v belonging to the set $\{\epsilon_a\epsilon_b, \epsilon_b\epsilon_c, \epsilon_c\epsilon_a, 1\}$, where the particular value depends on the behavior of π at v (see Figure 3.2 for an illustration of the four possibilities at a black vertex). We now assign weights to the edges of the Fisher graph $\mathbb{F}_n$ in such a way that the corresponding dimer configuration has the same weight as π.

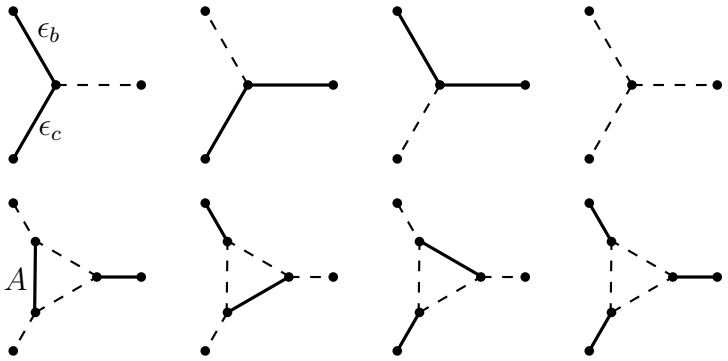

FIGURE 3.2. To each local polygon configuration at a black vertex of $\mathbb{H}_n$, there corresponds a dimer configuration on the Fisher graph $\mathbb{F}_n$. The situation at a white vertex is similar. In the leftmost configuration, the local weight of the polygon configuration is $\epsilon_b\epsilon_c$, and in the dimer configuration A.

Each edge of a Fisher triangle has one of the types: vertical (denoted 'v'), NE/SW (denoted 'ne'), or NW/SE (denoted 'nw'), according to its orientation. To each edge e of $\mathbb{F}_n$ lying in a Fisher triangle, we allocate the weight:

$$\begin{aligned} &A \quad \text{if } e \text{ is vertical (v)},\\ &B \quad \text{if } e \text{ is NE/SW (ne)},\\ &C \quad \text{if } e \text{ is NW/SE (nw)}, \end{aligned}$$

where A, B, C satisfy (3.6)–(3.7). The dimer partition function is given by

$$Z_n(D) := \sum_D A^{|D(\mathrm{v})|} B^{|D(\mathrm{ne})|} C^{|D(\mathrm{nw})|}, \tag{3.9}$$

where $D(s) \subseteq D$ is the set of dimers of type s. It is immediate, by inspection of Figure 3.2, that

$$Z_n(D) = Z_n,$$

and that the correspondence $\pi \leftrightarrow D$ is weight-preserving.

3.5. **The spectral curve of the dimer model.** We turn now to the spectral curve of the weighted dimer model on $\mathbb{F}_n$, for the background to which the reader is referred to [13]. The fundamental domain of $\mathbb{F}_n$ is drawn in Figure 3.3, and the edges of $\mathbb{F}_n$ are oriented as in that figure. It is easily checked that this orientation is 'clockwise odd', in the sense that any face of $\mathbb{H}_n$, when traversed clockwise, contains an odd number of edges oriented in the corresponding direction. The fundamental domain

has 6 vertices labelled $1, 2, \ldots, 6$, and its weighted adjacency matrix (or 'Kasteleyn matrix') is the 6×6 matrix $W = (k_{i,j})$ with

$$k_{i,j} = \begin{cases} w_{i,j} & \text{if } \langle i, j \rangle \text{ is oriented from } i \text{ to } j, \\ -w_{i,j} & \text{if } \langle i, j \rangle \text{ is oriented from } j \text{ to } i, \\ 0 & \text{if there is no edge between } i \text{ and } j, \end{cases}$$

where the $w_{i,j}$ are as indicated in Figure 3.3. From W we obtain a *modified* adjacency (or 'modified Kasteleyn') matrix K as follows.

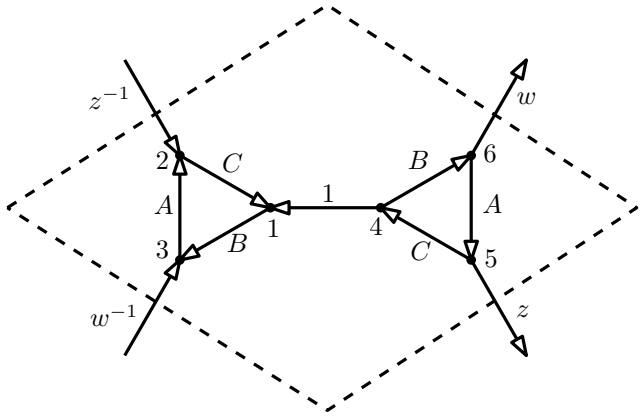

FIGURE 3.3. Weighted 1×1 fundamental domain of $\mathbb{F}_n$. The vertices are labelled $1, 2, \ldots, 6$, and the weights $w_{i,j}$ and orientations are as indicated. The further weights $w^{\pm 1}$, $z^{\pm 1}$ are as indicated.

We may consider the graph of Figure 3.3 as being embedded in a torus, that is, we identify the upper left boundary and the lower right boundary, and also the upper right boundary and the lower left boundary, as illustrated in the figure by dashed lines.

Let $z, w \in \mathbb{C}$ be non-zero. We orient each of the four boundaries of Figure 3.3 (denoted by dashed lines) from their lower endpoint to their upper endpoint. The 'left' and 'right' of an oriented portion of a boundary are as viewed by a person traversing in the given direction.

Each edge $\langle u, v \rangle$ crossing a boundary corresponds to two entries in the weighted adjacency matrix, indexed (u, v) and (v, u). If the edge starting from u and ending at v crosses an upper-left/lower-right boundary from left to right (respectively, from right to left), we modify the adjacency matrix by multiplying the entry (u, v) by z (respectively, z^{-1}). If the edge starting from u and ending at v crosses an upper-right/lower-left boundary from left to right (respectively, from right to left), in the modified adjacency matrix, we multiply the entry by w (respectively, w^{-1}). We

modify the entry (v,u) in the same way. For a definitive interpretation of Figure 3.3, the reader is referred to the matrix following.

The signs of these weights are chosen to reflect the orientations of the edges. The resulting *modified adjacency matrix* (or 'modified Kasteleyn matrix') is

$$K = \begin{pmatrix} 0 & -C & B & -1 & 0 & 0 \\ C & 0 & -A & 0 & -z^{-1} & 0 \\ -B & A & 0 & 0 & 0 & -w^{-1} \\ 1 & 0 & 0 & 0 & -C & B \\ 0 & z & 0 & C & 0 & -A \\ 0 & 0 & w & -B & A & 0 \end{pmatrix}.$$

The *characteristic polynomial* is given (using Mathematica or otherwise) by

$$\begin{aligned} P(z,w) &:= \det K \\ &= 1 + A^4 + B^4 + C^4 + (A^2C^2 - B^2)\left(w + \frac{1}{w}\right) \\ &\quad + (A^2B^2 - C^2)\left(z + \frac{1}{z}\right) + (B^2C^2 - A^2)\left(\frac{w}{z} + \frac{z}{w}\right). \end{aligned} \tag{3.10}$$

By (3.6) and (2.8),

$$\begin{aligned} P(z,w) &= 1 + \alpha^2\beta^2 + \alpha^2\gamma^2 + \beta^2\gamma^2 + \alpha^2\gamma^2(\beta^2 - 1)\left(w + \frac{1}{w}\right) \\ &\quad + \alpha^2\beta^2(\gamma^2 - 1)\left(z + \frac{1}{z}\right) + \beta^2\gamma^2(\alpha^2 - 1)\left(\frac{w}{z} + \frac{z}{w}\right). \end{aligned}$$

The *spectral curve* is the zero locus of the characteristic polynomial, that is, the set of roots of $P(z,w) = 0$. It will be useful later to identify the intersection of the spectral curve with the unit torus $\mathbb{T}^2 = \{(z,w) : |z| = |w| = 1\}$.

Let

$$\begin{aligned} U &= \alpha\beta + \beta\gamma + \gamma\alpha - 1, \\ V &= -\alpha\beta + \beta\gamma + \gamma\alpha + 1, \\ S &= \alpha\beta - \beta\gamma + \gamma\alpha + 1, \\ T &= \alpha\beta + \beta\gamma - \gamma\alpha + 1. \end{aligned} \tag{3.11}$$

Proposition 3.3. *Let $\epsilon_a, \epsilon_b, \epsilon_c \neq 0$, so that $\alpha, \beta, \gamma > 0$. Either the spectral curve does not intersect the unit torus $\mathbb{T}^2$, or the intersection is a single real point of multiplicity 2. Moreover, the spectral curve intersects $\mathbb{T}^2$ at a single real point if and only if $UVST = 0$, where U, V, S, T are given by (3.11).*

Proof. The proof follows from a computation similar to those of [10, 12]. The details are omitted but the overview is as follows. First, it is proved that $P(z,w) \geq 0$ for $(z,w) \in \mathbb{T}^2$, and $P(z,w) = 0$ only when $(z,w) \in \{-1,1\}^2$. Moreover,

$$\begin{aligned} P(1,1) &= (-1 + A^2 + B^2 + C^2)^2 = U^2, \\ P(-1,-1) &= (1 - A^2 + B^2 + C^2)^2 = S^2, \\ P(-1,1) &= (1 + A^2 - B^2 + C^2)^2 = T^2, \\ P(1,-1) &= (1 + A^2 + B^2 - C^2)^2 = V^2, \end{aligned}$$

by (3.6). Since $A, B, C \neq 0$, no more than one of the above four numbers can equal zero. □

The condition $UVST \neq 0$ may be understood as follows. Let γ_i be given by (2.10), and note that

$$\gamma_2(\alpha^{-1}, \beta) = 1/\gamma_1(\alpha, \beta). \tag{3.12}$$

Proposition 3.4. *Let $\alpha, \beta, \gamma > 0$ and let U, V, S, T satisfy (3.11).*

(a) *We have that $UVST = 0$ if and only if $\gamma \in \{\gamma_1, \gamma_2\}$.*
(b) *The region R_{sup} of Theorem 2.2 is an open, connected subset of $(0,\infty)^3$.*
(c) *The region R_{sub} is the disjoint union of four open, connected subsets of $(0,\infty)^3$, namely,*

$$\begin{aligned} R^1_{\mathrm{sub}} &= \{\gamma < \gamma_1\} \cap \{\alpha\beta < 1\}, \quad R^2_{\mathrm{sub}} = \{\gamma < \gamma_1\} \cap \{\alpha\beta > 1\}, \\ R^3_{\mathrm{sub}} &= \{\gamma > \gamma_2\} \cap \{\alpha < \beta\}, \quad R^4_{\mathrm{sub}} = \{\gamma > \gamma_2\} \cap \{\alpha > \beta\}. \end{aligned} \tag{3.13}$$

Proof. Part (a) follows by an elementary manipulation of (3.11). Part (b) holds since $\gamma_1 < \gamma_2$ for all $\alpha, \beta > 0$. Part (c) is a consequence of the facts that $\gamma_1 = 0$ when $\alpha\beta = 0$, and $\gamma_2 = \infty$ when $\alpha = \beta$. □

4. Proof of Theorem 2.2

By Remark 2.1, we shall assume without loss of generality that $\epsilon_a, \epsilon_b, \epsilon_c > 0$. Let ℓ be the path of $A\mathbb{H}_n$ connecting Me and Mf as in (2.9). To a configuration $\pi \in \Pi_{e,f}$ we associate the configuration $\pi' := \pi + \ell \in \Pi^{\mathrm{poly}}$ (with addition modulo 2). The correspondence $\pi \leftrightarrow \pi'$ is one-to-one between $\Pi_{e,f}$ and Π^{poly}. By considering the configurations contributing to $Z_{n,e\leftrightarrow f}$, we obtain that

$$\frac{Z_{n,e\leftrightarrow f}}{Z_n(P)} = \left(\prod_{g \in \ell} \epsilon_g \right) \frac{Z_{n,\ell}(P)}{Z_n(P)}, \tag{4.1}$$

where $Z_{n,\ell}(P)$ is the partition function of polygon configurations on $A\mathbb{H}_n$ with the weights of g-type half-edges along ℓ changed from ϵ_g to ϵ_g^{-1}.

From the Fisher graph $\mathbb{F}_n$, we construct an *augmented Fisher graph* $A\mathbb{F}_n$ by placing two further vertices on each non-triangular edge of $\mathbb{F}_n$, see Figure 4.1. We will construct a weight-preserving correspondence between polygon configurations on $A\mathbb{H}_n$ and dimer configurations on $A\mathbb{F}_n$.

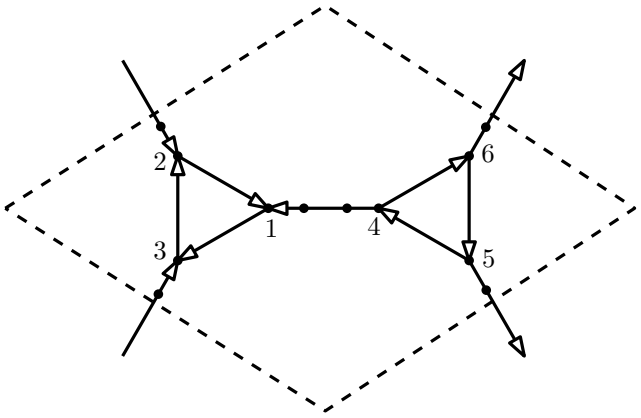

FIGURE 4.1. The fundamental domain of $A\mathbb{F}_n$, which may be compared with Figure 3.3.

We assign weights to the edges of $A\mathbb{F}_n$ as follows. Each triangular edge of $A\mathbb{F}_n$ is assigned weight 1. Each non-triangular g-type edge of the Fisher graph $\mathbb{F}_n$ is divided into three parts in $A\mathbb{F}_n$ to which we refer as the left edge, the middle edge, and the right edge. The left edge and right edges are assigned weight ϵ_g^{-1}, while the middle edge is assigned weight 1. We shall identify the characteristic polynomial P^A of this dimer model in the forthcoming Lemma 4.1.

There is a one-to-one correspondence between polygon configurations on $A\mathbb{H}_n$ and polygon configurations on $\mathbb{H}_n$. The latter may be placed in one-to-one correspondence with dimer configurations on $A\mathbb{F}_n$ as follows. Consider a polygon configuration π on $\mathbb{H}_n$. An edge $e \in E_n$ is present in π if and only if the corresponding middle edge of e is present in the corresponding dimer configuration $D = D(\pi)$ on $A\mathbb{F}_n$. Once the states of middle edges of $A\mathbb{F}_n$ are determined, they generate a unique dimer configuration on $A\mathbb{F}_n$.

By consideration of the particular situations that can occur within a given fundamental domain, one obtains that the correspondence is weight-preserving (up to a fixed factor), whence

$$Z_n(P) = Z_n(AD) \prod_{g \in AE_n} \epsilon_g,$$

where $Z_n(AD)$ is the partition function of the above dimer model on $A\mathbb{F}_n$. A similar dimer interpretation is valid for $Z_{n,\ell}(P)$, and thus we have

$$\frac{Z_{n,e\leftrightarrow f}}{Z_n(P)} = \left(\prod_{g\in\ell}\epsilon_g\right)\frac{Z_{n,\ell}(P)}{Z_n(P)} = \left(\prod_{g\in\ell}\epsilon_g^{-1}\right)\frac{Z'_n(AD)}{Z_n(AD)}, \tag{4.2}$$

where $Z'_n(AD)$ is the partition function for dimer configurations on $A\mathbb{F}_n$, in which the left and right non-triangular edges corresponding to half-edges in π have weight ϵ_g, and all the other left/right non-triangular edges have unchanged weights ϵ_g^{-1}.

We assign a clockwise-odd orientation to the edges of $A\mathbb{F}_n$ as indicated in Figure 4.1. The above dimer partition functions may be represented in terms of the Pfaffians of the weighted adjacency matrices corresponding to $Z_n(AD)$ and $Z'_n(AD)$. See [6, 7, 11, 19].

Recall that $A\mathbb{F}_n$ is a graph embedded in the $n \times n$ torus. Let γ_x and γ_y be two non-parallel homology generators of the torus, that is, γ_x and γ_y are cycles winding around the torus, neither of which may be obtained from the other by continuous movement on the torus. Moreover, we assume that γ_x and γ_y are paths in the dual graph that meet in a unique face and that cross disjoint edge-sets. For definiteness, we take γ_x (respectively, γ_y) to be the upper left (respectively, upper right) dashed cycles of the dual triangular lattice, as illustrated in Figure 4.2. We multiply the weights of all edges crossed by γ_x (respectively, γ_y) by z or z^{-1} (respectively, w or w^{-1}), according to their orientations.

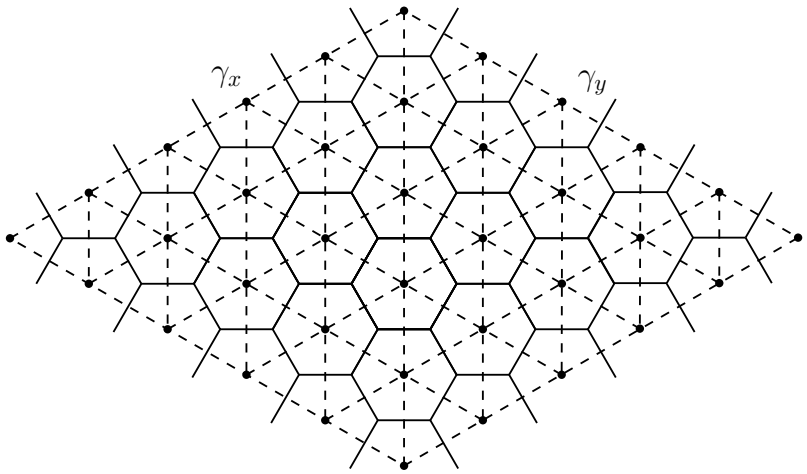

FIGURE 4.2. Two cycles γ_x and γ_y in the dual triangular graph of the toroidal graph $\mathbb{H}_n$. The upper left and lower right sides of the diamond are identified, and similarly for the other two sides.

Let $K_n(z,w)$ be the weighted adjacency matrix of the original dimer model above, and let $K_n'(z,w)$ be that with the weights of g-type edges along ℓ changed from ϵ_g^{-1} to ϵ_g.

If n is even, by (4.2) and results of [6, 11] and [16, Chap. IV],

(4.3)
$$\frac{Z_{n,e\leftrightarrow f}}{Z_n(P)} = \left(\prod_{g\in\ell}\epsilon_g^{-1}\right)\frac{-\mathrm{Pf}\,K_n'(1,1)+\mathrm{Pf}\,K_n'(-1,1)+\mathrm{Pf}\,K_n'(1,-1)+\mathrm{Pf}\,K_n'(-1,-1)}{-\mathrm{Pf}\,K_n(1,1)+\mathrm{Pf}\,K_n(-1,1)+\mathrm{Pf}\,K_n(1,-1)+\mathrm{Pf}\,K_n(-1,-1)}.$$

The corresponding formula when n is odd is

$$\frac{Z_{n,e\leftrightarrow f}}{Z_n(P)} = \left(\prod_{g\in\ell}\epsilon_g^{-1}\right)\frac{\mathrm{Pf}\,K_n'(1,1)+\mathrm{Pf}\,K_n'(-1,1)+\mathrm{Pf}\,K_n'(1,-1)-\mathrm{Pf}\,K_n'(-1,-1)}{\mathrm{Pf}\,K_n(1,1)+\mathrm{Pf}\,K_n(-1,1)+\mathrm{Pf}\,K_n(1,-1)-\mathrm{Pf}\,K_n(-1,-1)},$$

as explained in the discussion of 'crossing orientations' of [17, pp. 2192–2193]. The ensuing argument is essentially identical in the two cases, and therefore we may assume without loss of generality that n is even.

We shall make use of the fact that the Pfaffian and determinant of an antisymmetric matrix M satisfy $[\mathrm{Pf}\,(M)]^2 = \det(M)$, whence

$$\mathrm{Pf}\,(MM') = (-1)^j \mathrm{Pf}\,(M)\mathrm{Pf}\,(M'), \tag{4.4}$$

for some $j = j(M,M') \in \{0,1\}$.

Note that $K_n(\theta,\nu)$ and $K_n'(\theta,\nu)$ are antisymmetric when $\theta,\nu\in\{-1,1\}$. By (4.4), for $\theta,\nu\in\{-1,1\}$,

$$\begin{aligned}\frac{\mathrm{Pf}\,K_n'(\theta,\nu)}{\mathrm{Pf}\,K_n(\theta,\nu)} &= (-1)^j \mathrm{Pf}\,[K_n'(\theta,\nu)K_n^{-1}(\theta,\nu)] \\ &= (-1)^j \mathrm{Pf}\,\big[R_n K_n^{-1}(\theta,\nu) + I\big],\end{aligned} \tag{4.5}$$

where

$$R_n = K_n'(\theta,\nu) - K_n(\theta,\nu), \tag{4.6}$$

and j is an integer which depends on n but not on θ, ν.

The following argument is similar to that of [11, Thm 4.2]. In preparation, we define the 4×4 matrix

$$S_g = \begin{pmatrix} 0 & \epsilon_g - \epsilon_g^{-1} & 0 & 0 \\ \epsilon_g^{-1} - \epsilon_g & 0 & 0 & 0 \\ 0 & 0 & 0 & \epsilon_g - \epsilon_g^{-1} \\ 0 & 0 & \epsilon_g^{-1} - \epsilon_g & 0 \end{pmatrix},$$

for $g = a, b$.

Each half-edge of $\mathbb{H}_n$ along ℓ corresponds to an edge of $A\mathbb{F}_n$, namely, a left or right non-triangular edge. Moreover, the path ℓ has a periodic structure in $A\mathbb{H}_n$,

each period of which consists of four edges of $A\mathbb{H}_n$, namely, a NW/SE half-edge, followed by two horizontal half-edges, followed by another NW/SE half-edge. These four edges correspond to four non-triangular edges of $A\mathbb{F}_n$ with endpoints denoted $v_{b_3}, v_{b_4}, v_{a_1}, v_{a_2}, v_{a_3}, v_{a_4}, v_{b_1}, v_{b_2}$.

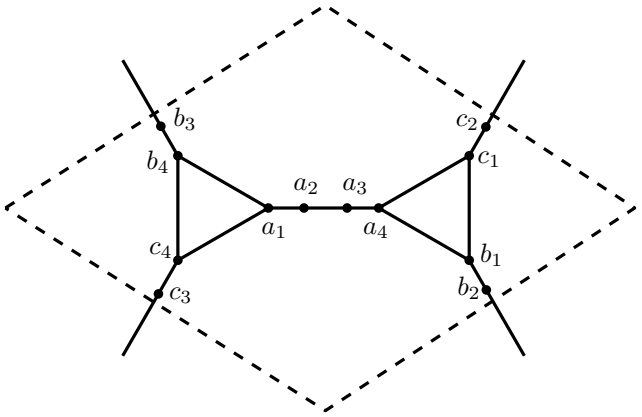

FIGURE 4.3. The fundamental domain of $A\mathbb{F}_n$ with vertex-labels.

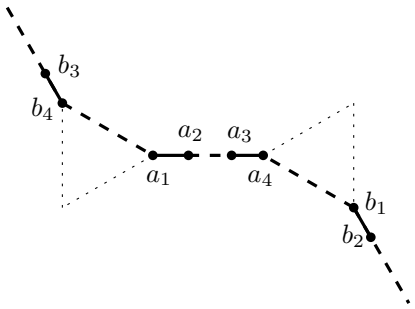

FIGURE 4.4. Part of the path ℓ between two NW/SE edges.

The graph $A\mathbb{F}_n$ may be regarded as $n \times n$ copies of the fundamental domain of Figure 4.1, with vertices labelled as in Figures 4.3–4.4. We index these by (p, q) with $p, q = 1, 2, \ldots, n$, and let $D_{p,q}$ be the fundamental domain with index (p, q). Let $\mathcal{D} = \{(p, q) : D(p, q) \cap \ell \neq \varnothing\}$, so that the cardinality of $\mathcal{D}$ depends only on $|e - f|$. Let $(p, q) \in \mathcal{D}$. The 12×12 block of R_n with rows and columns labelled by the vertices in $D_{p,q}$ may be written as

$$R_n(D_{p,q}, D_{p,q}) = \begin{pmatrix} S_a & 0 & 0 \\ 0 & -S_b & 0 \\ 0 & 0 & 0 \end{pmatrix}. \tag{4.7}$$

Each entry in (4.7) is a 4×4 block, and the rows and columns are indexed by $v_{a_1}, \ldots, v_{a_4}, v_{b_1}, \ldots, v_{b_4}, v_{c_1}, \ldots, v_{c_4}$. All other entries of R_n equal 0.

Owing to the special structure of R_n, it turns out that the Pfaffian of $S_n := R_n K_n^{-1}(\theta, \nu) + I$ is the same as the Pfaffian of a certain submatrix of S_n given as follows. From S_n, we retain all rows indexed by translations of the v_{a_i}, and all columns indexed by translations of the v_{b_j}. Since each fundamental domain contains four such vertices of each type, the resulting submatrix $S_n(e, f)$ is square with dimension $4|\mathcal{D}|$. By following the corresponding computations of [11, Sect. 4] and [16, Chap. VIII], we find that $\mathrm{Pf}\,(S_n) = \mathrm{Pf}\,(S_n(e, f))$.

Moreover, the limiting entries of $K_n^{-1}(\gamma, \tau)$ as $n \to \infty$ can be computed explicitly using the arguments of [9, Thm 4.3] and [8, Sects 4.2–4.4], details of which are omitted here:

$$\lim_{n\to\infty} K_n^{-1}(\theta, \nu)(D_{p_1,q_1}, v_r; D_{p_2,q_2}, v_s) = -\frac{1}{4\pi^2} \int_{|z|=1} \int_{|w|=1} z^{p_2-p_1} w^{q_2-q_1} K_1^{-1}(z, w)_{v_s,v_r} \frac{dz}{iz} \frac{dw}{iw}, \tag{4.8}$$

where p_1, q_1, p_2, q_2 are positive integers, and $r, s \in \{a_i, b_i : i = 1, 2, 3, 4\}$, and $K_1^{-1}(z, w)_{v_s,v_r}$ is the (v_s, v_r) entry of $K_1^{-1}(z, w)$. Note that the right side of (4.8) does not depend on the values of $\theta, \nu \in \{-1, 1\}$,

As in the above references, by (4.3) and (4.8), the (formal) limit $M(e, f) = \lim_{n\to\infty} M_n(e, f)$ exists and equals the Pfaffian of a block Toeplitz matrix with dimension depending on $|e - f|$, and with symbol ψ given by

$$\psi(\zeta) = \frac{1}{2\pi} \int_0^{2\pi} T(\zeta, \phi)\, d\phi, \tag{4.9}$$

where $T(\zeta, \phi)$ is the 8×8 matrix with rows and columns indexed by $v_{a_1}, v_{a_2}, v_{a_3}, v_{a_4}$, $v_{b_1}, v_{b_2}, v_{b_3}, v_{b_4}$ (with rows and columns ordered differently) given by

$$\begin{pmatrix} \epsilon_a^{-1} + K_1^{-1}(\zeta, e^{i\phi})_{v_{a_2},v_{a_1}} \lambda_a & K_1^{-1}(\zeta, e^{i\phi})_{v_{a_2},v_{a_2}} \lambda_a & \cdots & K_1^{-1}(\zeta, e^{i\phi})_{v_{a_2},v_{b_4}} \lambda_a \\ -K_1^{-1}(\zeta, e^{i\phi})_{v_{a_1},v_{a_1}} \lambda_a & \epsilon_a^{-1} - K_1^{-1}(\zeta, e^{i\phi})_{v_{a_1},v_{a_2}} \lambda_a & \cdots & -K_1^{-1}(\zeta, e^{i\phi})_{v_{a_1},v_{b_4}} \lambda_a \\ \vdots & \vdots & \ddots & \vdots \\ K_1^{-1}(\zeta, e^{i\phi})_{v_{b_3},v_{a_1}} \lambda_b & K_1^{-1}(\zeta, e^{i\phi})_{v_{b_3},v_{a_2}} \lambda_b & \cdots & \epsilon_b^{-1} + K_1^{-1}(\zeta, e^{i\phi})_{v_{b_3},v_{b_4}} \lambda_b \end{pmatrix},$$

and $\lambda_g = 1 - \epsilon_g^{-2}$.

One may write

$$[K_1^{-1}(z, w)]_{i,j} = \frac{Q_{i,j}(z, w)}{P^A(z, w)}, \tag{4.10}$$

where $Q_{i,j}(z, w)$ is a Laurent polynomial in z, w derived in terms of certain cofactors of $K_1(z, w)$, and $P^A(z, w) = \det K_1(z, w)$ is the characteristic polynomial of the dimer model.

Lemma 4.1. *The characteristic polynomial P^A of the above dimer model on $A\mathbb{F}_n$ satisfies $P^A(z,w) = (\epsilon_a\epsilon_b\epsilon_c)^{-4}P(z,w)$, where $P(z,w)$ is the characteristic polynomial of (3.10).*

Proof. The characteristic polynomial P^A satisfies $P^A(z,w) = \det K_1(z,w)$. Each term in the expansion of the determinant corresponds to an oriented loop configuration consisting of oriented cycles and doubled edges, with the property that each vertex has exactly two incident edges. It may be checked that there is a one-to-one correspondence between loop configurations on the two graphs of Figures 4.1 and 3.3, by preserving the track of each cycle and adding doubled edges where necessary. The weights of a pair of corresponding loop configurations differ by a multiplicative factor of $(ABC)^2 = (\epsilon_a\epsilon_b\epsilon_c)^4$. □

By the above, the limit $M(e,f)$ exists whenever $P^A(z,w)$ has no zeros on the unit torus $\mathbb{T}^2$. By Lemma 4.1 and Proposition 3.3, the last occurs if and only if $UVST \neq 0$. The proof of part (a) is complete, and we turn towards parts (b) and (c).

Consider an infinite block Toeplitz matrix J, viewed as the limit of an increasing sequence of finite truncated block Toeplitz matrices J_n. When the corresponding spectral curve does not intersect the unit torus, the existence of $\det J$ as the limit of $\det J_n$ is proved in [21, 22]. By Lemma 4.1 and Proposition 3.3, the spectral curve condition holds if and only if $UVST \neq 0$. Since the Pfaffian is a square root of the determinant, we deduce the existence of the limit

$$\Lambda(\alpha,\beta,\gamma) := \lim_{|e-f|\to\infty} \lim_{n\to\infty} \left(\frac{Z_{n,e\leftrightarrow f}}{Z_n(P)}\right)^2, \tag{4.11}$$

whenever $UVST \neq 0$.

By Proposition 3.3, the function Λ is defined on the domain $D := (0,\infty)^3 \setminus \{UVST = 0\}$. We may interpret Λ as the determinant of an infinite block Toeplitz matrix, and in this context we may extend the domain of Λ to a neighborhood of D in $\mathbb{C}^3$.

Lemma 4.2. *Assume $\alpha,\beta,\gamma > 0$. The function Λ is an analytic function of the complex variables α, β, γ except when $UVST = 0$, where U,V,S,T are given by (3.11).*

Proof. This holds as in the proofs of [11, Lemmas 4.4–4.7]. We consider Λ as the determinant of a block Toeplitz matrix, and use Widom's formula (see [21, 22], and also [5, Thm 8.7]) to evaluate this determinant. As in the proof of [5, Thm 8.7], Λ can be non-analytic only if the spectral curve intersects the unit torus, which is to say (by Lemma 4.1 and Proposition 3.3) if $UVST = 0$. □

The equation $UVST = 0$ defines a surface in the first octant $(0,\infty)^3$, whose complement is a union of five open, connected components (see Proposition 3.4). By Lemma 4.2, Λ is analytic on each such component. It follows that, on any such component: either $\Lambda \equiv 0$, or Λ is non-zero except possibly on a nowhere dense set.

Let $\alpha, \beta, \gamma > 0$. By Proposition 3.4, $UVST \neq 0$ if and only if

$$\gamma \in (0, \gamma_1) \cup (\gamma_1, \gamma_2) \cup (\gamma_2, \infty), \tag{4.12}$$

where the γ_i are given by (2.10).

Proof of part (b). By Proposition 3.4, $UVST \neq 0$ on the open, connected region R_{sup}. Therefore, Λ is analytic on R_{sup}. Hence, either $\Lambda \equiv 0$ on R_{sup}, or $\Lambda \not\equiv 0$ on R_{sup} and the zero set $Z := \{r = (\alpha, \beta, \gamma) \in R_{\text{sup}} : \Lambda(r) = 0\}$ is nowhere dense in R_{sup}. It therefore suffices to find $(\alpha, \beta, \gamma) \in R_{\text{sup}}$ such that $\Lambda(\alpha, \beta, \gamma) \neq 0$.

Consider the 1-2 model of Sections 3.1–3.3 with $a = b > 0$ and $c > 4a$. By (2.8), (3.5), and (3.6), the corresponding polygon model has parameters

$$\alpha = \beta = \frac{c - 2a}{c + 2a}, \qquad \gamma = \frac{c^2}{(c - 2a)(c + 2a)}.$$

In this case, $\gamma_2 = \infty$ and $\gamma \in (\gamma_1, \gamma_2)$.

By [5, Thm 3.1(b)], for almost every such c, the 1-2 model has non-zero long-range order. By Lemma 3.2, $\Lambda(\alpha, \beta, \gamma) \neq 0$ for such c.

Proof of part (c). By the remarks concerning the Ising model at the end of Section 2.1, when $\alpha, \beta, \gamma > 0$ are sufficiently small, the two-edge correlation function $M(e, f)$ of the polygon model equals the two-spin correlation function $\langle \sigma_e \sigma_f \rangle$ of a ferromagnetic Ising model on $A\mathbb{H}$ at high temperature. Since the latter has zero long-range order, it follows that $\Lambda = 0$. Suppose, in addition, that $\alpha\beta < 1$ and $\gamma < \gamma_1$. Since Λ is analytic on R^1_{sub} (in the notation of (3.13)), we deduce that $\Lambda \equiv 0$ on R^1_{sub}. We next extend this conclusion to R^k_{sub} with $k = 2, 3, 4$.

Let $\pi \in \Pi^{\text{poly}}$ be a polygon configuration on $A\mathbb{H}_n$, and let $\pi' \in \Pi^{\text{poly}}$ be obtained from π by

$$\pi'(e) = \begin{cases} \pi(e) & \text{if } e \text{ is NW/SE,} \\ 1 - \pi(e) & \text{otherwise.} \end{cases}$$

Let $w^{\alpha,\beta,\gamma}(\pi)$ be the weight of π as in (2.5), with parameters α, β, γ. Then

$$w^{\alpha,\beta,\gamma}(\pi) = \frac{1}{\alpha^{\#a}\gamma^{\#c}} w^{\alpha^{-1},\beta,\gamma^{-1}}(\pi'), \tag{4.13}$$

where $\#g$ is the number of g-type edges in $\mathbb{H}_n$. Similarly, (4.13) holds for $\pi, \pi' \in \Pi_{e,f}$.

Let $(\alpha, \beta, \gamma) \in R^4_{\text{sub}}$. By (3.12), we have that $\alpha^{-1}\beta < 1$ and $\gamma^{-1} < \gamma_1(\alpha^{-1}, \beta)$, so that $(\alpha^{-1}, \beta, \gamma^{-1}) \in R^1_{\text{sub}}$. By (4.13) with $\pi \in \Pi^{\text{poly}} \cup \Pi_{e,f}$,

$$\Lambda(\alpha, \beta, \gamma) = \Lambda(\alpha^{-1}, \beta, \gamma^{-1}) = 0.$$

Therefore, $\Lambda \equiv 0$ on R^4_{sub}.

Let π'' be obtained from π by

$$\pi''(e) = \begin{cases} \pi(e) & \text{if } e \text{ is NE/SW,} \\ 1 - \pi(e) & \text{otherwise,} \end{cases}$$

so that (4.13) holds with $(\alpha^{-1}, \beta, \gamma^{-1})$ replaced by $(\alpha^{-1}, \beta^{-1}, \gamma)$ on the right side, and an amended denominator.

Let $(\alpha, \beta, \gamma) \in R^2_{\text{sub}}$, whence $(\alpha^{-1}, \beta^{-1}, \gamma) \in R^1_{\text{sub}}$ by (3.12). As above,

$$\Lambda(\alpha, \beta, \gamma) = \Lambda(\alpha^{-1}, \beta^{-1}, \gamma) = 0,$$

whence $\Lambda \equiv 0$ on R^2_{sub}. The case of R^3_{sub} can be deduced as was R^4_{sub}.

Acknowledgements

This work was supported in part by the Engineering and Physical Sciences Research Council under grant EP/103372X/1. ZL acknowledges support from the Simons Foundation under grant #351813.

References

[1] R. J. Baxter, *Exactly Solved Models is Statistical Mechanics*, Academic Press, London, 1982.
[2] H. Duminil-Copin, R. Peled, W. Samotij, and Y. Spinka, *Exponential decay of loop lengths in the loop $O(n)$ model with large n*, (2014), to appear.
[3] G. R. Grimmett and S. Janson, *Random even graphs*, Electron. J. Combin. **16** (2009), Paper R46, 19 pp.
[4] G. R. Grimmett and Z. Li, *The 1-2 model: dimers, polygons, the Ising model, and phase transition*, (2015), http://arxiv.org/abs/1507.04109.
[5] ———, *Critical surface of the 1-2 model*, (2015), http://arxiv.org/abs/1506.08406.
[6] P. W. Kasteleyn, *The statistics of dimers on a lattice, I. The number of dimer arrangements on a quadratic lattice*, Physica **27** (1961), 1209–1225.
[7] ———, *Dimer statistics and phase transitions*, J. Math. Phys. **4** (1963), 287–293.
[8] R. Kenyon, *Local statistics of lattice dimers*, Ann. Inst. H. Poincaré, Probab. Statist. **33** (1997), 591–618.
[9] R. Kenyon, A. Okounkov, and S. Sheffield, *Dimers and amoebae*, Ann. Math. **163** (2006), 1019–1056.
[10] Z. Li, *Local statistics of realizable vertex models*, Commun. Math. Phys. **304** (2011), 723–763.
[11] ———, *Critical temperature of periodic Ising models*, Commun. Math. Phys. **315** (2012), 337–381.
[12] ———, *1-2 model, dimers and clusters*, Electron. J. Probab. **19** (2014), 1–28.
[13] ———, *Spectral curves of periodic Fisher graphs*, J. Math. Phys. **55** (2014), Paper 123301, 25 pp.
[14] ———, *Uniqueness of the infinite homogeneous cluster in the 1-2 model*, Electron. Commun. Probab. **19** (2014), 1–8.
[15] K. Y. Lin and F. Y. Wu, *General vertex model on the honeycomb lattice: equivalence with an Ising model*, Modern Phys. Lett. B **4** (1990), 311–316.

[16] B. McCoy and T. T. Wu, *The Two-Dimensional Ising Model*, Harvard University Press, Cambridge MA, 1973.
[17] M. Schwartz and J. Bruck, *Constrained codes as networks of relations*, IEEE Trans. Inform. Th. **54** (2008), 2179–2195.
[18] H. N. V. Temperley and M. E. Fisher, *Dimer problem in statistical mechanics—an exact result*, Philos. Mag. **6** (1961), 1061–1063.
[19] G. Tesler, *Matchings in graphs on non-orientable surfaces*, J. Combin. Theory Ser. B **78** (2000), 198–231.
[20] B. L. van der Waerden, *Die lange Reichweite der regelmässigen Atomanordnung in Mischkristallen*, Zeit. Physik **118** (1941), 473–488.
[21] H. Widom, *On the limit of block Toeplitz determinants*, Proc. Amer. Math. Soc. **50** (1975), 167–173.
[22] ———, *Asymptotic behavior of block Toeplitz matrices and determinants. II*, Adv. Math. **21** (1976), 1–29.

Statistical Laboratory, Centre for Mathematical Sciences, Cambridge University, Wilberforce Road, Cambridge CB3 0WB, UK
E-mail address: g.r.grimmett@statslab.cam.ac.uk,
URL: http://www.statslab.cam.ac.uk/~grg/

Department of Mathematics, University of Connecticut, Storrs, Connecticut 06269-3009, USA
E-mail address: zhongyang.li@uconn.edu
URL: http://www.math.uconn.edu/~zhongyang/